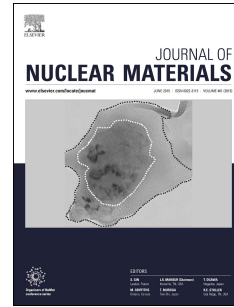# Journal Pre-proof

The effect on the mechanical response of Cr and Ni segregation on dislocation lines in bcc Fe

M.I. Pascuet, G. Bonny, G. Monnet, L. Malerba

Please cite this article as: M.I. Pascuet, G. Bonny, G. Monnet, L. Malerba, The effect on the mechanical response of Cr and Ni segregation on dislocation lines in bcc Fe, *Journal of Nuclear Materials* (2020), doi: https://doi.org/10.1016/j.jnucmat.2020.152319.

This is a PDF file of an article that has undergone enhancements after acceptance, such as the addition of a cover page and metadata, and formatting for readability, but it is not yet the definitive version of record. This version will undergo additional copyediting, typesetting and review before it is published in its final form, but we are providing this version to give early visibility of the article. Please note that, during the production process, errors may be discovered which could affect the content, and all legal disclaimers that apply to the journal pertain.

The effect on the mechanical response of Cr and Ni segregation on dislocation lines in bcc Fe

M.I. Pascuet[a*], G. Bonny[b], G. Monnet[c] and L. Malerba[d]

[a]*Materials Department, CONICET-CNEA – Godoy Cruz 2290 – (C1425FQB) CABA– Argentine*
[b]*Nuclear Materials Science Institute, SCK CEN – Boeretang 200 – (2400) Mol – Belgium*
[c]*EDF – R&D, MM - Avenues des Renardières - 77680 Moret sur Loing–France*
[d]*Energy Materials Division, CIEMAT – Avda. Complutense 40, 28040 Madrid – Spain*

ABSTRACT

The understanding of irradiation-induced strengthening in ferritic-martensitic high-Cr steels remains an essential issue in the assessment of materials for fusion and next generation fission reactors. Recent advanced experimental studies revealed the importance of solute-rich clusters, containing Cr, Ni, Si, P and Mn, which often are created as a consequence of segregation at dislocation lines. In this work, Metropolis Monte Carlo (MMC) is applied to investigate segregation of Cr and Ni atoms around edge dislocation lines in bcc Fe. The content of Cr is varied between 7% - 10%, with and without 0.25% of Ni. Molecular dynamics has subsequently been applied to the enriched dislocation lines to study the critical resolved shear stress at 300 K and 600 K for different concentrations of solutes in the alloy. It is found that even small amounts of Ni significantly increase the hardening of the material.

1. Introduction

Ferritic-martensitic high-Cr steels are commonly proposed as structural materials for advanced nuclear reactors (GenIV) and fusion devices. These steels are corrosion resistant and have a high resistance to swelling compared to for example austenitic steels [1 - 3]. Neutron irradiation is known to harden and embrittle these structural steels when used below about 400ºC, thereby limiting the lifetime of the components. This hardening and embrittlement is attributed to the interaction of dislocation lines with a number of microstructural features that are known to be produced under irradiation in these steels, namely: α' precipitates, dislocation loops, voids (if present) and irradiation-induced

---

* pascuet@cnea.gov.ar

CrNiSiPMn clusters that are believed to precipitate on loops [4 - 15]. In recent years, the contribution of these defects to the hardening has been investigated by simulating their interaction with dislocation lines. The interaction of (edge/screw) dislocations with Cr-rich precipitates was extensively studied in [14, 16 - 17]. The interaction of dislocation (edge/screw) lines with (1/2<111> and <100>) loops in bcc Fe were also extensively studied in [18] and the results could be used to assess by comparison the effect of solute decoration, by studying Cr enriched loops in [19 - 20], and CrNi enriched loops in [21]. Some integrated models haves been reported on the effects of the different radiation features (solid solution, dislocation loops, α' precipitates) on the yield stress [22]. But in these approaches, based on the dispersed barrier hardening model, the question of heterogeneous precipitation, i.e. on dislocations, are not tackled. As discussed in [23], this issue can be of primary importance in the presence of static aging as a consequence of the reduced mobility of matrix dislocations that are heavily decorated by solute atoms. This effect has been found to be important in the case of alloys that mimic reactor pressure vessel steels, as reported by Pascuet *et al.* [24 - 25] who confirmed that edge as well as screw matrix dislocations subjected to strong segregation are most likely to remain immobile during loading. So far, however, no studies have been devoted to estimate the increase in critical stress for a dislocation line to move when not only Cr, but also a minor alloying solute element that is present in F/M steels, such as Ni, is found to segregate at it. In this work, we therefore perform Metropolis Monte Carlo (MMC) simulations to simulate the segregation of Cr and Ni to an edge dislocation (ED) line. The resulting configuration is then used in molecular dynamics (MD) simulations to investigate its effect on the dislocation mobility. The increase in critical resolved shear stress is compared to simulations from the literature to put the results in perspective.

2. Computational details

2.1 Exchange Monte Carlo

A simulation box with an ED is generated in a crystallite with the normal axes x, y and z oriented as the [111], $[\bar{1}\bar{1}2]$ and $[1\bar{1}0]$ directions (Fig. 1). The dimensions of the box are 15 x 34 x 15 nm, corresponding to approximately 6×10^5 atoms of Fe-bcc. The Burgers vector is $\mathbf{b} = a_0/2$ [111], where a_0 is the corresponding lattice parameter, and the dislocation

line lies along the $[\bar{1}\bar{1}2]$ direction. The lattice parameters for each composition and temperature were calculated for a perfect bcc crystal without ED in the (N,P,T) ensemble, with the solute atoms randomly distributed in an Fe atom matrix (Table 1). The compositions that have been studied are: Fe with 7%Cr and 10%Cr, with and without 0.25%Ni. These compositions have been chosen because 7-14% is roughly the range of variation of the Cr content in F/M steels for nuclear applications, 8-9% being the most common composition. To minimize the interference of Cr precipitation with segregation, however, concentrations above 10% should be avoided. Thus, by choosing 7 and 10 %Cr we took two different concentrations that are both of relevance and unaffected by significant Cr precipitation. The small Ni content is in turn representative of the content of any minor solute in F/M steels.

Segregation around dislocations was studied at two temperatures, T_{seg}, namely room temperature, 300 K, and 600 K. These temperatures have been chosen because, while room temperature acts as a customary reference, 600 K is close to the typical reactor operation temperature in current fission reactors, especially in materials testing reactor irradiation campaigns, from where most experimental data come. It is also the temperature of a hypothetical future water-cooled fusion reactors and is below the rough threshold of 400ºC, above which experimentally no significant radiation hardening is generally measured. After thermalization, the free energy of the system of atoms was minimized by means of exchange MC sampling in the canonical ensemble (N,V,T), as implemented in LAMMPS [33], i.e. by rearranging the atomic species, using the EAM interatomic potential proposed by Bonny *et al.* [34 - 35]. Periodic boundary conditions were applied in the x and y directions. Along the z direction, in contrast, free surfaces limit the crystallite. Two atomic layers of 12 Å thickness, located at the bottom and the top of the crystal and parallel to the dislocation glide plane, limit the region where the atoms are exchanged, which lies between these two blocks as in a sandwich: this avoids precipitation at the free surfaces. The decision on the acceptance of the new configuration is based on the standard Metropolis Monte Carlo algorithm [36]. The convergence of each simulation was reached in 2×10^6 MC steps. For each possible pair of atom types, 100 exchanges were performed every 50 MD steps. The computing time per simulation using two machines was about 10^3 hours.

Table 1: Lattice parameters (Å).

	T_{seg} = 300 K	T_{seg} = 600 K	DFT/exp (T=0 K)	Potential (T = 0 K)
Fe-10Cr-0.25Ni	2.867	2.876		
Fe-10Cr	2.864	2.873		
Fe-7Cr-0.25Ni	2.867	2.876		

Fe-7Cr	2.865	2.873		
Fe-0.25Ni	2.859	2.867		
Fe (bcc)			2.869[a]/2.866[b]	2.855[f]
Ni (bcc)			2.801[c]	2.769[f]
Cr (bcc)			2.834[d]/2.878[e]	2.866[f]

[a] [28], [b] [29],[c] [30], [d] [31], [e] [32] and [f] [34 - 35]

2.2. Stress-strain curve calculation by MD

Once the equilibrium configurations with solute segregation have been obtained, simple shear strain is applied in a classical MD simulation at a constant $10^7 s^{-1}$ strain rate, at two stress-strain temperatures, T_{st}, namely 300 and 600 K. The simulations were performed in the micro-canonical ensemble (N,V,E) using the lattice parameters determined in Table 1. The resulting dislocation density in this set-up is $33 \times 10^{15} m^{-2}$. Two atomic blocks of 20 Å thickness, parallel to the dislocation glide plane, i.e., normal to the z axis, are fixed. Periodic boundary conditions along [111] and $[\bar{1}\bar{1}2]$ (x and y) are implemented. Shear strain is applied by displacing the upper layer of the simulation box in the direction of the Burgers vector and the corresponding resolved shear stress induced by the applied deformation is calculated as $\sigma_{xy} = F_x/A_{xy}$, where F_x is the total force in the x direction and A_{xy} is the xy cross section area [37].

3. Results

3.1. Solute precipitation around dislocations

In both binary Fe-Cr alloys, the segregation of Cr atoms is observed clearly at $T_{seg} = 300$ K, but very little at $T_{seg} = 600$ K, and in both cases only in the tensile region of the dislocation core. At 300 K, some Cr atoms also cluster away from the dislocation core, consistently with the Fe-Cr phase diagram predicted by the potential [38]. These results are also consistent with the observations by Zhurkin *et al.* [17, 23]. When Ni is added to the alloys, Cr atoms still segregate in the tensile zone of the dislocation core, while Ni atoms gather only in the compressed zone, for both Fe-10%Cr-0.25%Ni and Fe-7%Cr-0.25%Ni, consistently with observations by Bonny *et al.* [23]. This suggests that the interatomic potential describes Cr atoms as slightly oversized and Ni atoms as undersized. DFT and

experimental data (Table 1) show that Ni atoms in a bcc lattice behave as undersized atoms compared to bcc Fe. The employed potential also reproduces this effect. For Cr, the DFT and experimental data are opposite: DFT data suggest that Cr behaves as an undersized atom, while experimental data suggest that Cr behaves as oversized. However, both DFT and experiment show that the lattice parameter difference between bcc Fe and bcc Cr is very small. The employed potential predicts bcc Cr to be oversized compared to bcc Fe, but with a small difference, consistently with the experiment. Therefore, the fact that Ni segregates in the compressed zone, while Cr segregates in the tensile zone of the edge dislocation is a consequence of the fact that the potential reproduces correctly, based on the best available knowledge (experiment for bcc Cr, DFT for bcc Ni) the relative size of Cr, Fe and Ni atoms in the bcc lattice. Experimentally, precipitation under thermal ageing conditions in Fe-Cr alloys is observed to occur first at dislocations and only later in the bulk [39], thus the tendency to segregate (and later precipitate) at dislocation lines, rather than away from them, is correctly reproduced by the potential. Representative cases are shown in Fig. 1: (*a*) Fe-10%Cr and (*b*) Fe-10%Cr-0.25%Ni obtained at T_{seg} = 300 K (for practical reasons only a portion of the total box in the *y* direction is shown). Fig. 2 shows the *xy* section for all cases at 600 K.
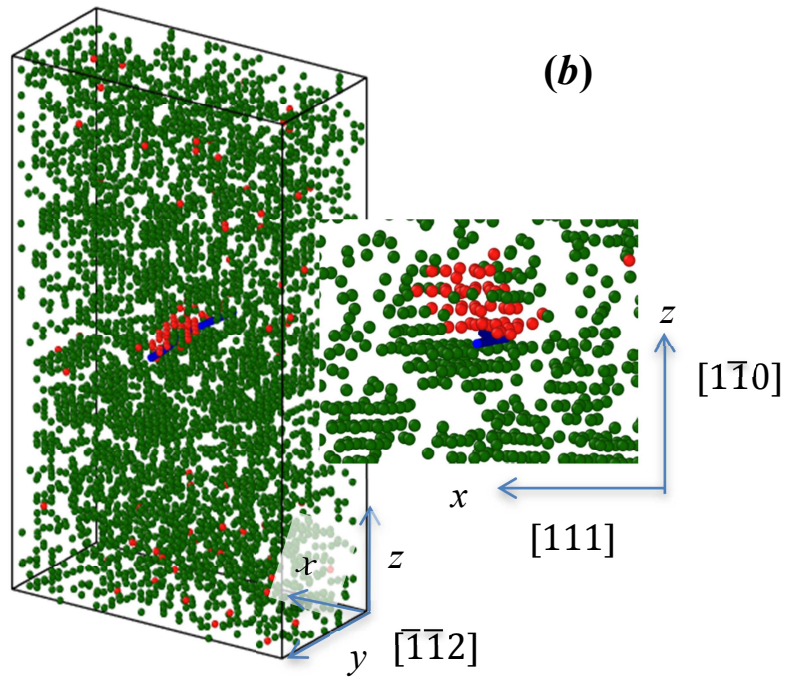
(b)
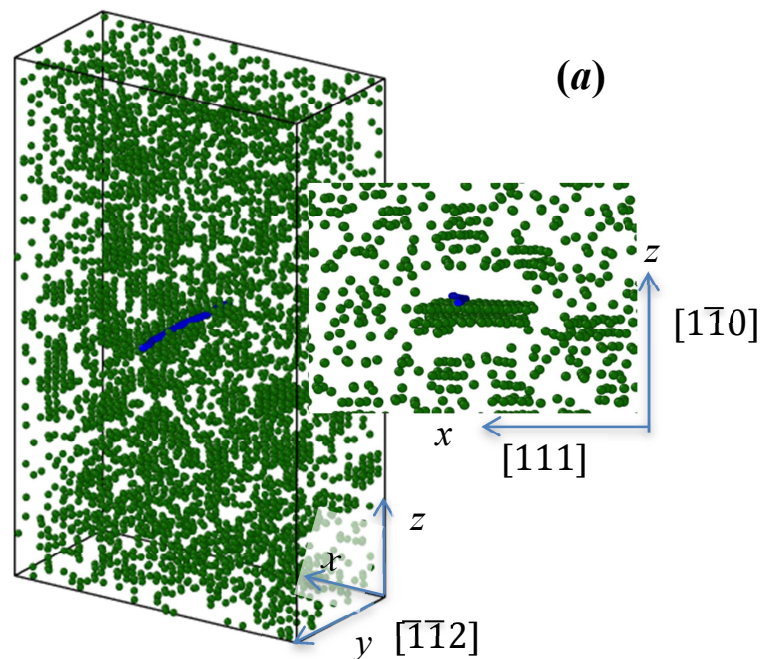
Fig. 1: Distribution of solutes in presence of an edge dislocation: (*a*) Fe-10%Cr, (*b*) Fe-10%Cr-0.25%Ni at T_{seg} = 300 K [26-27].
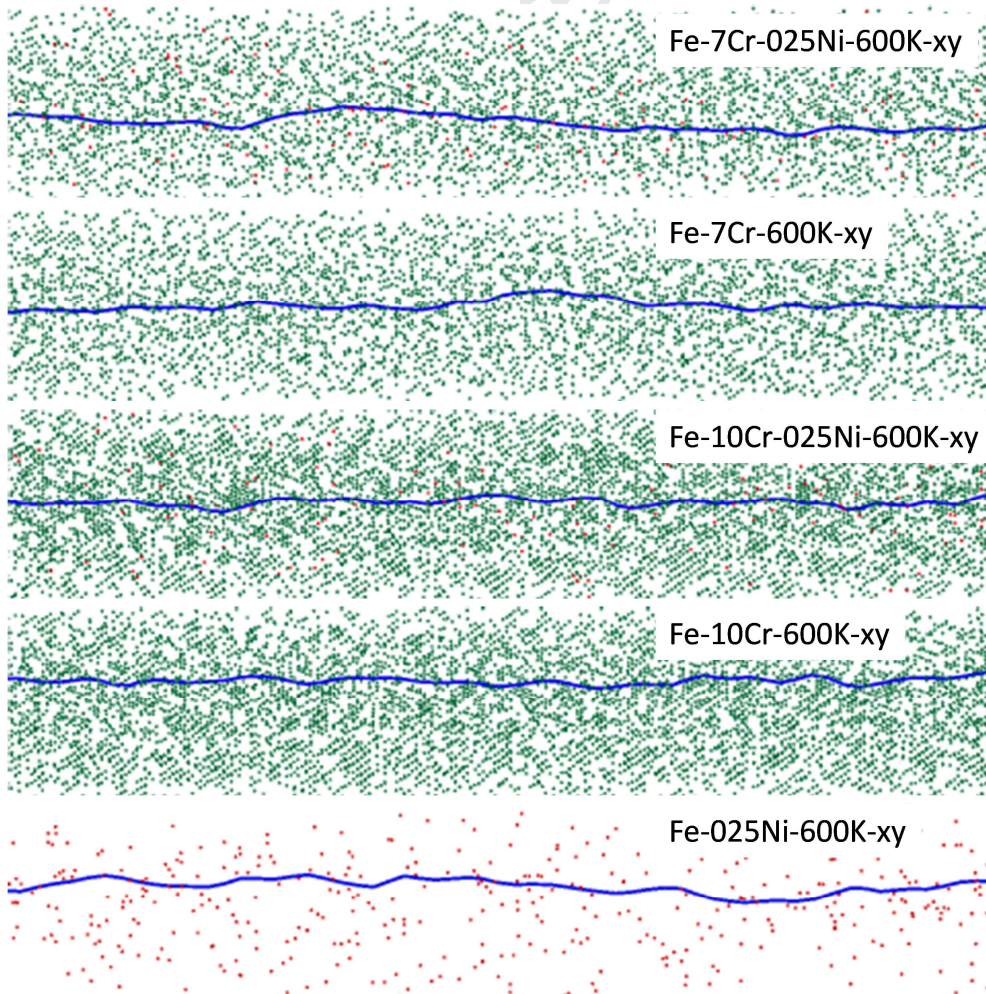
Fig. 2: Dislocation configurations decorated at 600 K by Cr and/or Ni atoms in the different alloys. Green atoms: Cr, red atoms: Ni, dislocation line in blue (Fe atoms are not shown for clarity).

To quantify the segregation around the dislocation core, concentration profiles were constructed, by calculating Cr and/or Ni concentrations in cylindrical slices around the dislocation line, increasing the radius of each of those cylinders by a_0. The concentration of Cr is shown in Fig. 3a (T_{seg} = 300 K) and 3b (T_{seg} = 600 K), of Ni in Fig. 4a (T_{seg} = 300 K) and 4b (T_{seg} = 600 K). Near the dislocation line, the segregated content is separated into two regions: concentration in the tensile zone, and concentration in the compressed zone. Outside the core, we observe that some small clusters of Cr are formed at 300 K. This is illustrated by the small oscillations in the concentration profile. However, most Cr segregated at the dislocation line.

When comparing the systems with or without 0.25%Ni, it is important to note that, despite the physical separation between the two species, the presence of Ni atoms does affect the precipitation of Cr, as we can see in Fig. 3a and b. The percentage of Cr near the dislocation core decreases when Ni atoms are present, both at 300 K and 600 K. To isolate the behavior of Ni atoms, we did simulations in Fe-0.25%Ni, at 300 K. We found that also in this case Ni atoms precipitate in the compressed zone on the dislocation core. The amount of Ni at the dislocation core is the highest in the absence of Cr, while it decreases by adding Cr, although the trend is not linear and depends on temperature. This indicates that there is also some influence of Cr on Ni segregation, although probably weaker, in the presence of a dislocation line. In contrast, in a system without dislocation, it has been shown that, if Ni is present, it has no influence on the Cr solubility [34].

Compared to the equilibrium binary phase diagrams corresponding to the potential, we conclude that the presence of the dislocation raises the solubility curve for Ni, inducing heterogeneous precipitation. For Fe-Cr, however, we cannot conclude the same. Our results indicate that the solubility limit with and without dislocation is unaltered. This finding is consistent with the work of [34].
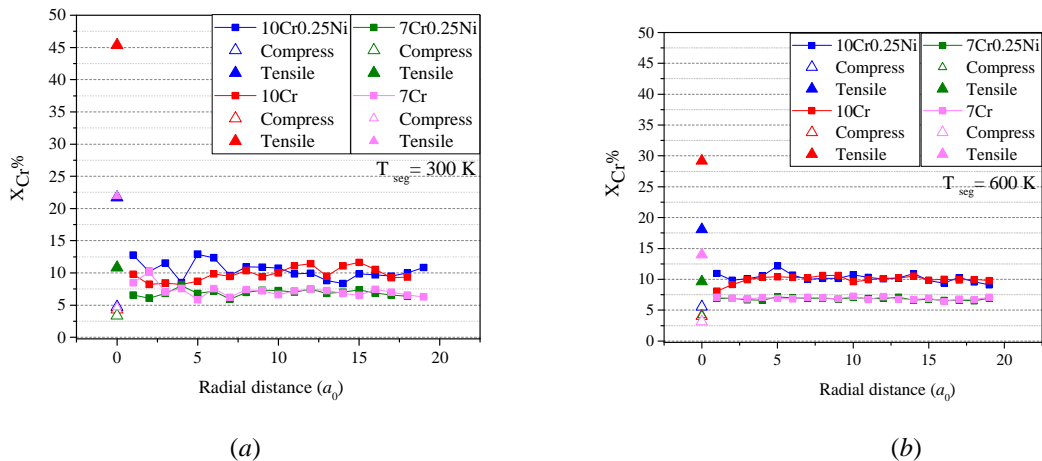

(a)   (b)

Fig. 3. Concentration profiles of Cr around the edge dislocation in the Fe-10%Cr-0.25%Ni (blue), Fe-10%Cr (red), Fe-7%Cr-0.25%Ni (green) and Fe-7%Cr (pink), segregation temperature (*a*) T_{seg} = 300 and (*b*) 600 K. The

dislocation line is placed at layer number = 0. The concentration in the compressed (tensile) zone of the core is represented by empty (full) triangles.
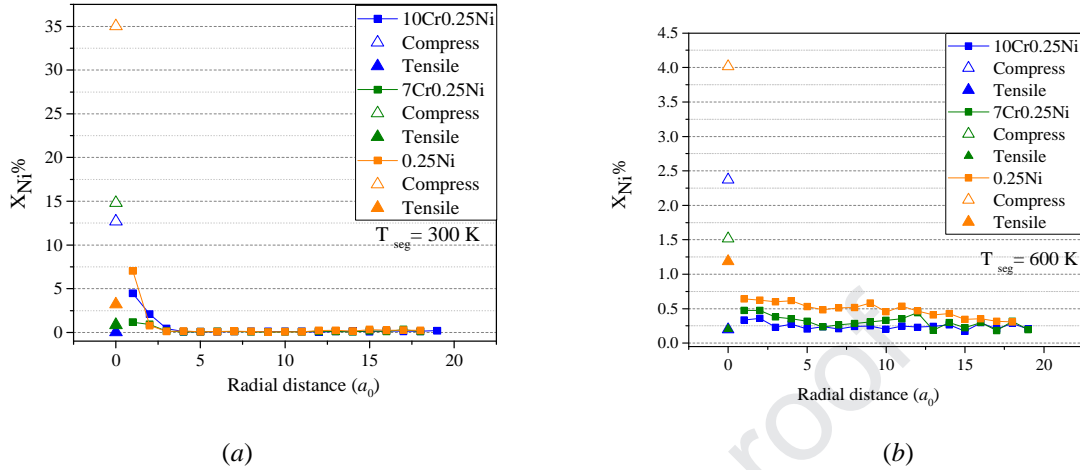

(a)   (b)

Fig. 4. Concentration profiles of Ni around the edge dislocation in the Fe-10%Cr-0.25%Ni (blue), Fe-7%Cr-0.25%Ni (green) and Fe-0.25%Ni (orange), segregation temperature (a) T_{seg} = 300 and (b) 600 K. The dislocation line is placed at layer number = 0. Concentration in compressed (tensile) zone of the core is represented by empty (full) triangles.

3.2. Effect on the mobility of edge dislocations

In this section, the configurations obtained by MMC are used to perform MD simulations, where the crystallite is loaded under simple shear strain to study the dislocation unpinning at two test temperatures (T_{st}): 300 K and 600 K. The methodology applied for the simulation is fairly standard and is described in [24 - 25]. A detailed comparison of the loading curves for the different configurations is presented in Fig. 5a (T_{st} = 300K) and Fig. 5b (T_{st} = 600K) for the alloys segregated at 300 K; and Fig. 6a (T_{st} = 300K) and Fig. 6b (T_{st} = 600K) for the alloys segregated at 600 K. The shape of the curves is the same for all cases, an elastic build-up of the stress due to the pinning of the dislocation, with a sharp decrease when the dislocation unpins from the segregated solute clusters. The unpinning stress (or the critical stress) for all investigated alloys is given in Table 2.
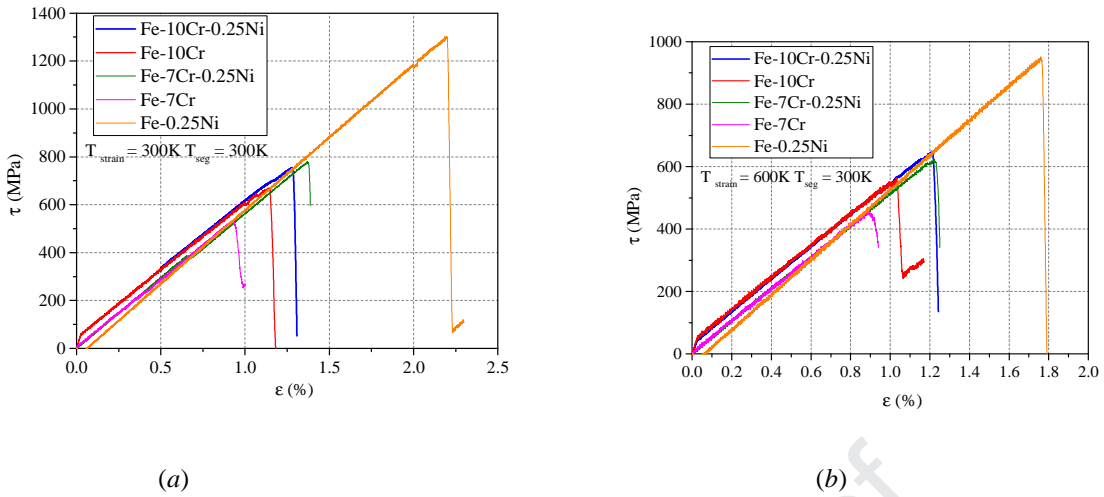
8

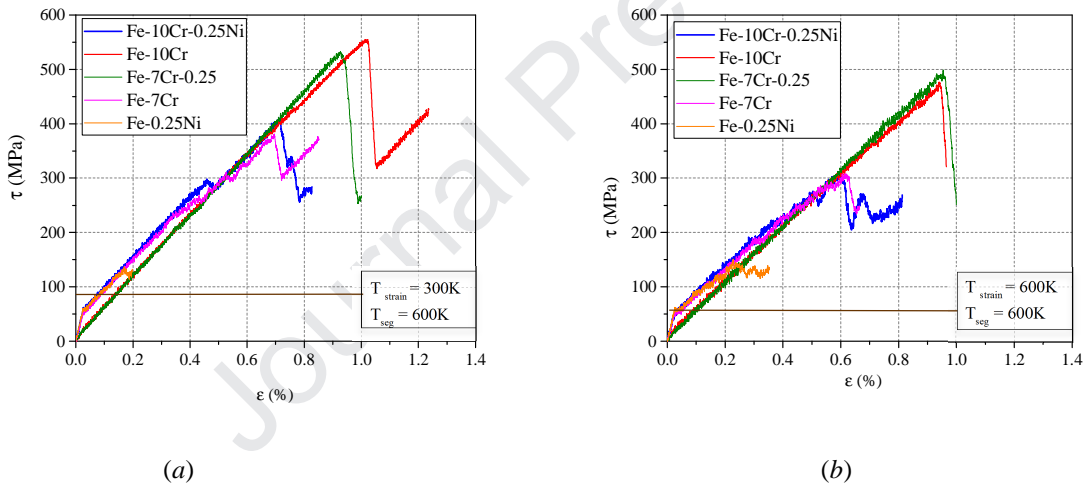(a)   (b)

Fig. 5. Stress-strain curves for edge dislocations in BCC Fe with different concentrations of Cr and Ni, (*a*) T_{st}= 300 K and (*b*) T_{st}= 600 K. (T_{seg} = 300 K).

(a)   (b)

Fig. 6. Stress-strain curves for edge dislocations in BCC Fe with different concentrations of Cr and Ni (*a*) T_{st} = 300 K and (*b*) T_{st} = 600 K. (T_{seg} = 600 K). The averaged friction stress for Fe-10Cr-0.25Ni system is represented by a brown straight line.

It is possible to isolate the net effect of segregation by subtracting the friction stress of the solid solution from the unpinning stress. Before segregation, Cr and Ni are randomly distributed in the matrix in a solid solution. When the dislocation moves, it encounters a diffuse resistance due to the distorsion of the matrix by individual Cr and Ni atoms. We call this resistance friction stress. To compute the latter, we made MD simulations of the edge dislocation moving through the corresponding alloy with all solute atoms randomly distributed. The computed average stress necessary to move the dislocation is recorded as the

9

friction stress and given in Table 2, as well, for 300 K and 600 K. The values for Fe-10%Cr are somewhat lower than the values published by Terentyev *et al.* [18], because the Fe-Cr interatomic potential is different, although for Fe-7%Cr the values are similar [40]. Once the friction stress is subtracted, the net increase in obstacle strength due to the pinning, $\Delta\sigma_C$, can be compared to other pinning mechanisms (see the following section) [18].

Table 2: Maximum shear stress (MPa) at 300K and 600K, friction stress (averaged value (MPa)).

	T_{seg} = 300K		T_{seg} = 600K			
	T_{st}= 300K	T_{st} = 600K	T_{st} = 300K	T_{st} = 600K	T_{st} = 300K	T_{st} = 600K
	τ_{max}	τ_{max}	τ_{max}	τ_{max}	Friction	Friction
Fe-10Cr-0.25Ni	757	645	410	315	89	53
Fe-10Cr	668	560	553	472	76	46
Fe-7Cr-0.25Ni	777	618	532	491	82	50
Fe-7Cr	534	470	381	307	64	39
Fe-0.25Ni	1295	946	161	148	20	10

To help correlate $\Delta\sigma_C$ to the observed segregation at the dislocation core, all results are summarized in Fig.7. In the squares, the dislocation core is represented by a circle, where the top part is the compressed zone and the bottom part the tensile zone. The local concentration of Ni and Cr in the respective zones of the core is indicated. All the circles represent zones with the same diameter (1.5 nm). The $\Delta\sigma_C$ for each configuration is also indicated in the figure. The highest values of $\Delta\sigma_C$, are attained in alloys where Ni is present and segregated, at T_{seg}=300 K. Even with this very little amount of Ni (0.25%), the hardening effect is remarkable. The effect of Ni is even more pronounced when the Cr content decreases, making the Fe-7%Cr-0.25%Ni the most hardened alloy at 300 K. The hardening in the case of alloys segregated at 600 K, is the highest for Fe-10%Cr and Fe-7%Cr-0.25%Ni. In these cases the presence of Ni seems to have an opposite effect: it increases the unpinning stress in the case of the Fe-7%Cr alloy, while it decreases it in the case of the Fe-10Cr.
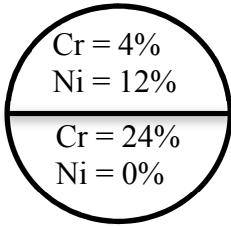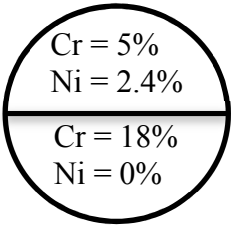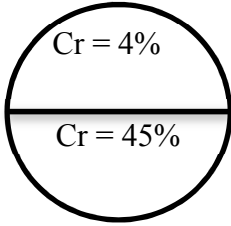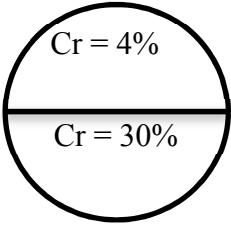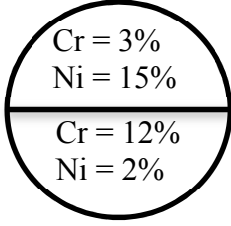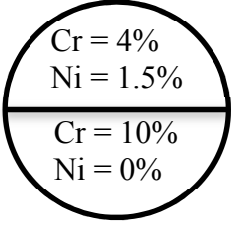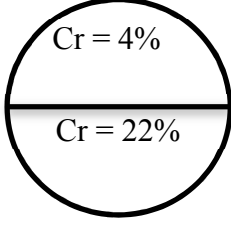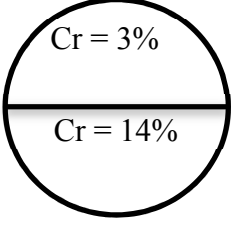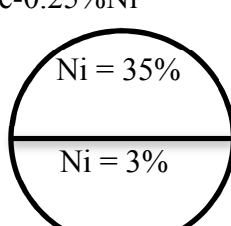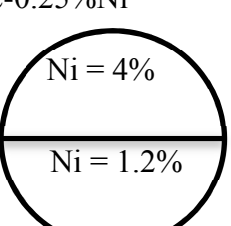
T_{seg} = 300K		T_{seg} = 600K	
$\Delta\tau_{MAX}$ (T_{st} = 300K)	$\Delta\tau_{MAX}$ (T_{st} = 600K)	$\Delta\tau_{MAX}$ (T_{st} = 300K)	$\Delta\tau_{MAX}$ (T_{st} = 600K)

Fe-10%Cr-0.25%Ni
Cr = 4%
Ni = 12%
Cr = 24%
Ni = 0%
668 MPa 592 MPa

Fe-10%Cr-0.25%Ni
Cr = 5%
Ni = 2.4%
Cr = 18%
Ni = 0%
321 MPa 262 MPa

Fe-10%Cr
Cr = 4%
Cr = 45%
592 MPa 514 MPa

Fe-10%Cr
Cr = 4%
Cr = 30%
477 MPa 426 MPa

Fe-7%Cr-0.25%Ni
Cr = 3%
Ni = 15%
Cr = 12%
Ni = 2%
695 MPa 568 MPa

Fe-7%Cr-0.25%Ni
Cr = 4%
Ni = 1.5%
Cr = 10%
Ni = 0%
450 MPa 441 MPa

Fe-7%Cr
Cr = 4%
Cr = 22%
470 MPa 431 MPa

Fe-7%Cr
Cr = 3%
Cr = 14%
317 MPa 268 MPa

Fe-0.25%Ni
Ni = 35%
Ni = 3%
1275 MPa 936 MPa

Fe-0.25%Ni
Ni = 4%
Ni = 1.2%
141 MPa 138 MPa

11

Fig. 7. Summary of the Ni and Cr concentration in the dislocation core for different temperatures (T_{seg}). The maximum stress is also indicated. In bold (normal) are the values for the results obtained at stress-strain temperature (T_{st}): 300 K (600 K).

4. Discussion

Our results confirm that in the investigated alloys the random solid solution of Cr and Ni atoms is not stable, especially in the presence of dislocations. Solutes segregated on the dislocation line are, however, not uniformly distributed, as would be expected in the case of Cottrell atmosphere. The clustering tendency generates strong heterogeneity in the distribution of solutes and even precipitates. With these clusters on the dislocation, the energy landscape is expected to vary strongly, thus creating attractive and repulsive poles. This is why the relaxed dislocation is no longer a straight line and follows the segregation relief in its slip plane (*xy*), as can be seen in Fig 2*c*. The dislocation is trapped in its position, which explains the large stresses for unpinning the dislocation computed in MD.

The values of the critical stress given in Table 2 can be rationalized as follows. In correspondence of the segregation produced at 600 K, the addition of Ni decreases or increases the unpinning stress, depending on the Cr content, (higher in Fe-10%Cr than in Fe-10%Cr-0.25%Ni; lower in Fe-7%Cr than in Fe-7%Cr-0.25%Ni). In contrast, at T_{seg} = 300 K, Ni has a clear hardening effect. It is therefore argued the difference in the unpinning stress between the Fe-10%Cr, Fe-10%Cr-0.25%Ni and Fe-7%Cr-0.25%Ni after segregation at 600 K is not significant and is related to the fact that at this higher temperature the segregation of Ni is limited, so its hardening effect is diluted with respect to the lower segregation temperature and the overall pinning stress is in this case more sensitive to the way in which especially Cr solutes, that are present in large concentration, arrange themselves along the dislocation line.

The correlation of hardening with Ni is clearly indicated by the somewhat surprisingly large pinning effect of this element in the Fe-0.25%Ni alloy. On the other hand, the strong hardening induced by Ni in bcc Fe has been revealed also in experimental investigations [41]. The computed values for segregation at 300 K are about 1 GPa, indicating that these decorated dislocations are immobile within classical loading conditions. Even for segregation at 600 K, the unpinning stress exceeds 150 MPa, which is equivalent to almost 450 MPa in the case of tensile deformed polycristals of Fe-0.25%Ni. This also suggests that, if Ni

segregates on dislocations, free dislocations must be nucleated in order to accommodate the deformation. The reasoning here is as follows. To have an idea of the consequence of such unpinning stress on the behaviour of a real alloy in a tensile test, we can estimate to a good approximation the corresponding macroscopic strengthening using the Taylor polycrystal model, which connects the critical resolved stress τ_c with the yield stress σ_y : $\Delta\sigma_y \approx M \Delta\tau_c$, where M is the Taylor factor, close to 2.7 for the BCC structure [42]. Since the segregation of Ni raises the stress necessary to move the dislocation from 20 MPa (random solid solution) to 161 MPa (segregated state), the corresponding yield stress increases from 54 MPa to 435 MPa, i.e. causes a strengthening of 381 MPa, thereby producing an amplification of the strengthening. Therefore, if Ni segregates on dislocations, free dislocations must be certainly nucleated in order to accommodate the plastic deformation.

The maximum stress values obtained here are compared in Fig. 8 (for the Fe-Cr and Fe-Cr-Ni systems) with some results from the literature: voids and Cr precipitates, as well as undecorated, Cr enriched and Cr-Ni enriched, <001> and ½<111> loops. The obstacle spacings between defects included in the figure correspond to: from 21 to 41 nm for voids, 21 nm for loops and from 41.4 to 61.8 nm for precipitates. These values are in the range of experimental observations. The shaded area in the upper part of the graph contains the results of this work and reveals that the resistance to dislocation motion due to solute segregation on the dislocation line is stronger than the effect of voids, loops and precipitates of size < 5 nm. Only above 5 nm in diameter does the obstacle strength of those defects become comparable to, though still smaller than, the effect of solute segregation on the dislocation line. We therefore conclude that, besides the classical hardening mechanisms through a field of obstacles (voids, precipitates and loops), the pinning of dislocation lines by solute segregation yields an important contribution to the hardening.

It is worth noting that, in principle, variations in the specific atomic distribution of solutes along the dislocation lines could affect the numerical value of the unpinning stress that we derived in this work. Logically, this presumption would dictate to perform a detailed sensitivity study, sampling a number of equilibrium configurations with the exchange MMC tool. However, with this MMC tool the equilibrium atomic distribution is mainly determined by the energetically favourable positions for solutes inherent to the dislocation, rather than on where the solutes were initially positioned. Furthermore, given the length of the considered dislocation line, a certain amount of inhomogenities (different size/density) of solute clusters spontaneously form along the dislocation line. Therefore, in practice, the resulting critical resolved

shear stress as we derived in this work can reasonably be considered as an effective averaged value over multiple different local solute environments along the dislocation line.
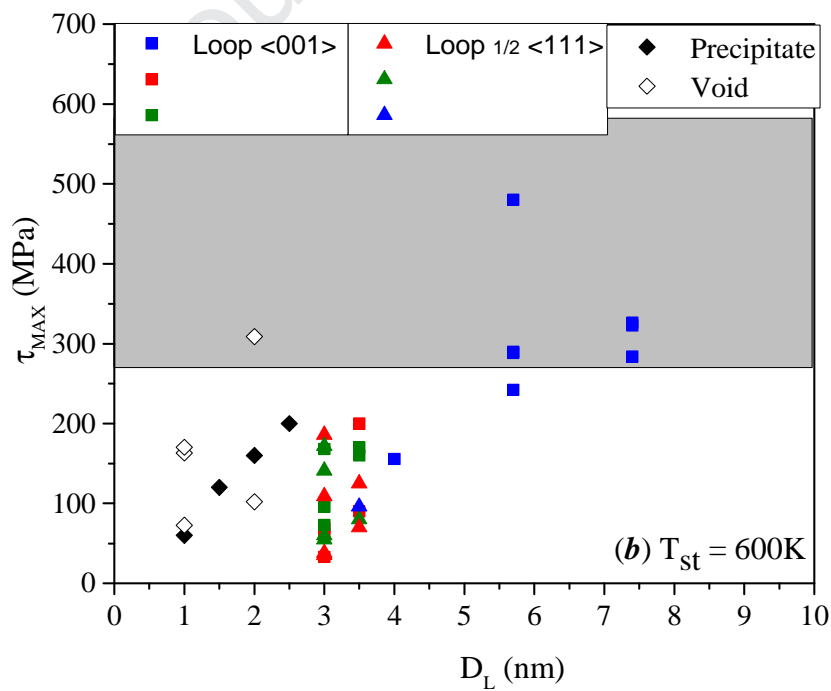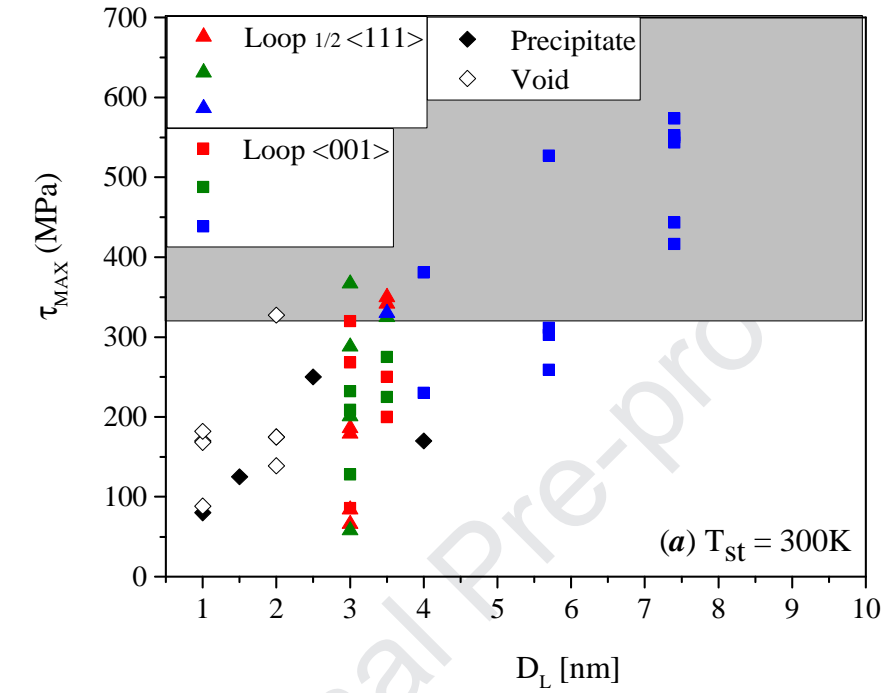
Fig. 8. Comparison in terms of maximum edge dislocation obstacle strength between radiation-produced defects, precipitates and solute decoration of the dislocation, as function of size (obtained from Fig. 3 and 4). (*a*) $T_{st} = 300$ K and (*b*) $T_{st} = 600$ K. The data from the literature concern undecorated [19 – 21, 43], Cr enriched [20, 21], and CrNi enriched [21] <001> and 1/2<111> loops; Cr precipitates [18, 44], and voids [43 - 46]. Colour code for loops, red: Cr enriched, green: CrNi enriched, blue: undecorated. The shaded zone contains the results of this work, for T=300 K (between = 317 and 695 MPa) and T=600 K (between = 262 and MPa).

5. Summary and conclusions

We studied Cr and Ni segregation near an edge dislocation line using exchange Monte Carlo at 300 and 600 K. We found significant enrichment of the dislocation core by Cr in the tensile zone and by Ni in the compressed zone. The combination of Ni and Cr together revealed a synergy leading to a reduced segregation in the dislocation core compared to the binaries separately.

MD simulations of the resulting configurations of the MMC simulations show that both Cr and Ni lead to significant hardening. We found that the hardening by solute segregation is largely affected by the small amount of added Ni.

When comparing this strengthening mechanism to the pinning of a moving dislocation line by voids, loops and precipitates, we find the latter to be weaker for sizes < 5 nm. Above 5 nm, the obstacle strength for voids, precipitates and loops is similar to the hardening observed through solute segregation on the dislocation line. Given these large unpinning stresses, the matrix dislocations are immobile in usual loading conditions and thus new dislocations must be generated during plastic deformation of these alloys.

Acknowledgements

References

[1]   L.K. Mansur, A.F. Rowcliffe, R.K. Nanstad, S.J. Zinkle, W.R. Corwin, R.E. Stoller, J. Nucl. Mater. 329-333 (2004) 166.
[2]   C. Fazio, A. Alamo, A. Almazouzi, S. de Grandis, D. Gomez-Briceno, J. Herry, L. Malerba, M. Rieth, J. Nucl. Mat. 392 (2009) 216.
[3]   C. Fazio, D.G. Briceno, M. Rieth, A. Gessi, J. Henry, L. Malerba, Nucl. Eng. Des. 241 (2011) 3514.
[4]   G.R. Odette, Scripta Metall. 17 (1983) 1183.
[5]   G.R. Odette, G.E. Lucas, J. Min. Metall. Mater. Soc. 53 (2001) 18.
[6]   G.R. Odette, C.L. Liu, B.D. With, Mater. Res. Soc. Symp. Proc. 439 (1997) 457.
[7]   C.A. English, W.J. Phytian, R.J. McElroy, Mater. Res. Soc. Symp. Proc. 439 (1997) 471.
[8]   P. Pareige, J.C. Van Duysen, P. Auger, App. Surf. Sci. 67 (1993) 342.
[9]   E. Meslin, B. Radiguet, P. Pareige, A. Barbu, J. Nucl. Mat. 399 (2010) 137.
[10]   E. Meslin, B. Radiguet, P. Pareige, C. Toffolon, A. Barbu, Exp. Mech. 51 (2011) 1453.
[11]   V. Kuksenko, C. Pareige, C. Genevois, F. Cuvilly, M. Roussel, P. Pareige, J. Nucl. Mat. 415 (2011) 61.
[12]   V. Kuksenko, C. Pareige, P. Pareige, J. Nucl. Mat. 425 (2012) 125.
[13]   V. Kuksenko, C. Pareige, P. Pareige, J. Nucl. Mat. 432 (2013) 160.
[14]   C. Pareige, V. Kuksenko, P. Pareige, J. Nucl. Mat. 456 (2013) 471.
[15]   L. Malerba, G. Bonny, D. Terentyev, E.E. Zhurkin, M. Hou, K. Vörtler, K. Nordlund, J. Nucl. Mat. 442 (2013) 486.
[16]   D. Terentyev, G. Bonny, L. Malerba, J. Nucl. Mat. 386 (2009) 257.
[17]   E.E. Zhurkin, D. Terentyev, M. Hou, L. Malerba, G. Bonny, J. Nucl. Mat. 417 (2011) 1082.
[18]   D. Terentyev, G. Bonny, C. Domain, G. Monnet, L. Malerba, J. Nucl. Mat. 442 (2013) 470.
[19]   D. Terentyev, F. Bergner, Y. Osetsky, Acta Mater. 61 (2013) 1444.
[20]   D. Terentyev, A. Bakaev, J. Phys.: Condens. Matter, 25 (2013) 265702.
[21]   G. Monnet, J. Nucl Mat. 508 (2018) 609–627.
[22]   F. Bergner, C. Pareige, M. Hernández-Mayoral, L. Malerba, C. Heintze, Journal of Nuclear Materials. 448 (2014) 96–102.
[23]   G. Bonny, A. Bakaev, D. Terentyev, E.E. Zhurkin, M. Posselt, J. Nucl. Mat. 498 (2018) 430.
[24]   M.I. Pascuet, E. Martínez, G. Monnet, L. Malerba, J. Nucl. Mat. 494 (2017) 311.
[25]   M.I. Pascuet, G. Monnet, G. Bonny, E. Martínez, J.J.H. Lim, M.G. Burke, L. Malerba, J. Nucl. Mat. 519 (2019) 265.
[26]   A. Stukowski, K. Albe, Modelling Simul. Mater. Sci. Eng. 18 (2010) 085001.
[27]   A. Stukowski, V.V. Bulatov, A. Arsenlis, Modelling Simul. Mater. Sci. Eng. 20 (2012) 085007
[28]   A. Hung, I. Yarovsky, J. Muscat, S. Russo, I. Snook, R.O. Watts, Surf. Sci. 501 (2002) 261.
[29]   N.W. Ashcroft, N.D. Mermin, Solid State Physics, Saunders College, 1976.
[30]   Y. Mishin, M.J. Mehl, D.A. Papaconstantopoulos, Acta Mater. 53 (2005) 4029.
[31]   P. Olsson, J. Wallenius, C. Domain, K. Nordlund and L. Malerba, Phys. Rev. B, 72 (2005) 214119.
[32]   W. Pearson, A Handbook of Lattice Spacings and Structures of Metals and Alloys, Pergamon Press, New York, 1958.
[33]   S. Plimpton, J. Comp. Phys. 117 (1995) 1.
[34]   G. Bonny, A. Bakaev, P. Olsson, C. Domain, E.E. Zhurkin, M. Posselt, J. Nucl. Mat. 484 (2017) 42.
[35]   G. Bonny, R.C. Pasianot, D. Terentyev, L. Malerba, Philos. Mag. 91 (2011) 1724.
[36]   M.P. Allen, D. Tildesley, Computer Simulation of Liquids, Claredon Press, Oxford, 1987.
[37]   Y.N. Osetsky, D.J. Bacon, Modelling Simul. Mater. Sci. Eng. 11 (2003) 427.
[38]   G. Bonny, R.C. Pasianot, E.E. Zhurkin, M. Hou, Comput. Mater. Sci. 50 (2011) 2216.
[39]   R. Lagneborg, Trans. ASM 60 (1967) 67.
[40]   S.M. Hafez Haghighat, D. Terentyev, R. Schäublin, J. Nucl. Mat. 417 (2011) 1094.
[41]   T. Tanaka, S. Watanabe, Acta Metall. 19 (1971) 991
[42]   J.M. Rosenberg, H.R. Piehler, Metall. Trans. 2 (1971) 257.
[43]   G. Bonny, D. Terentyev, J. Elena, A. Zinovev, B. Minov, E.E. Zhurkin, J. Nucl. Mat. 473 (2016) 283.
[44]   Y.N. Osetsky, D.J. Bacon, J. Nucl. Mat. 323 (2003) 268.
[45]   D. Terentyev, L. Malerba, G. Bonny, A.T. Al-Motasem, M. Posselt, J. Nucl. Mat. 419 (2011) 134.

[46]   D. Terentyev, D.J. Bacon, Y.N. Osetsky, J. Phys. Cond. Mat. 20 (2008) 445007.

Declaration of interests

☒The authors declare that they have no known competing financial interests or personal relationships that could have appeared to influence the work reported in this paper.

☐The authors declare the following financial interests/personal relationships which may be considered as potential competing interests: